Supporting Information for

Utilization of Structure-Based Design to Identify Novel, Irreversible Inhibitors of EGFR Harboring the T790M Mutation

Edward J. Hennessy,*,† Claudio Chuaqui,† Susan Ashton,‡ Nicola Colclough,‡ Darren A. E. Cross,‡ Judit É. Debreczeni,‡ Cath Eberlein,‡ Lakshmaiah Gingipalli,† Teresa C. M. Klinowska,‡ Jonathan P. Orme,‡ Li Sha,† and Xiaoyun Wu†

†*Oncology iMed, Innovative Medicines & Early Development, AstraZeneca R&D Boston, 35 Gatehouse Drive, Waltham, Massachusetts 02451, United States*
‡*Oncology iMed & Discovery Sciences, Innovative Medicines & Early Development, AstraZeneca, Mereside, Alderley Park, Macclesfield, Cheshire SK10 4TG, United Kingdom*

Contents

Analysis of EGFR WT vs. T790M/L858R Selectivity in Aminopyrazines

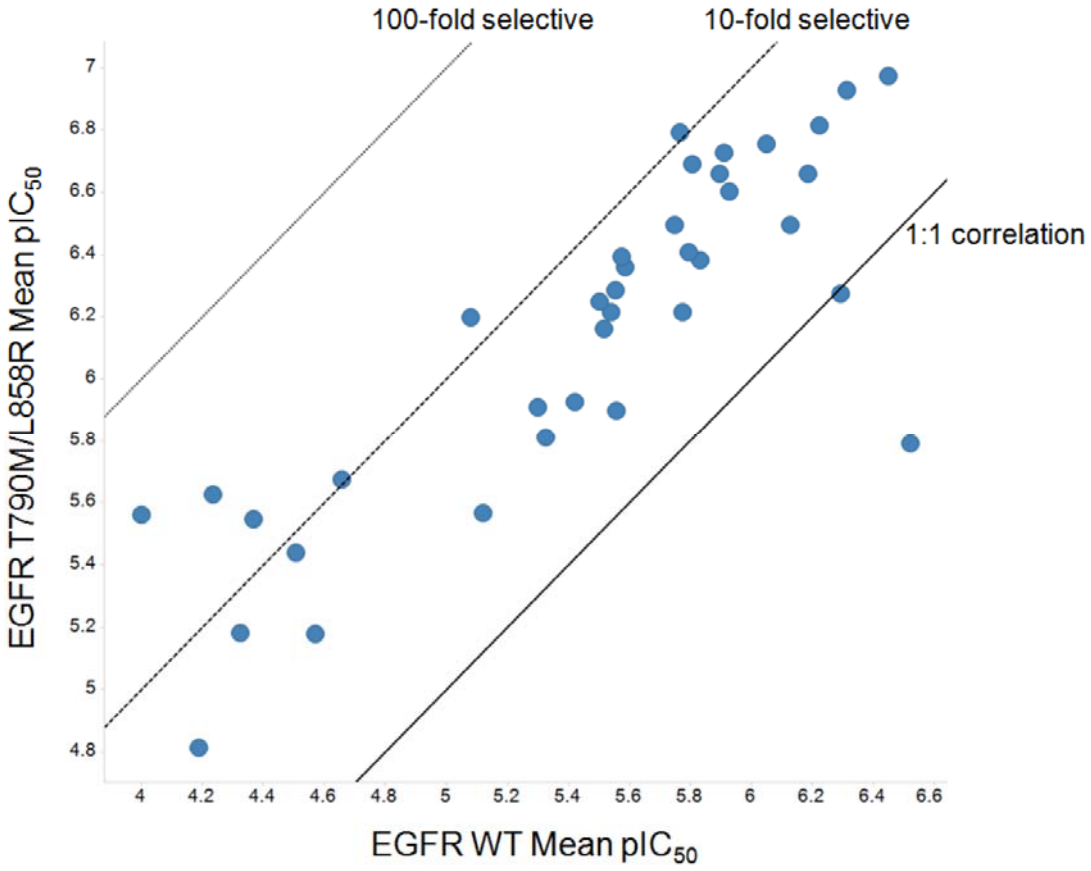

Figure S1. Comparison of EGFR WT and EGFR T790M/L858R potency for a selection of reversible compounds from aminopyrazine scaffold. In general, compounds are 5- to 10-fold selective for EGFR T790M/L858R over EGFR WT.

Structure-Based Design of Compound 5

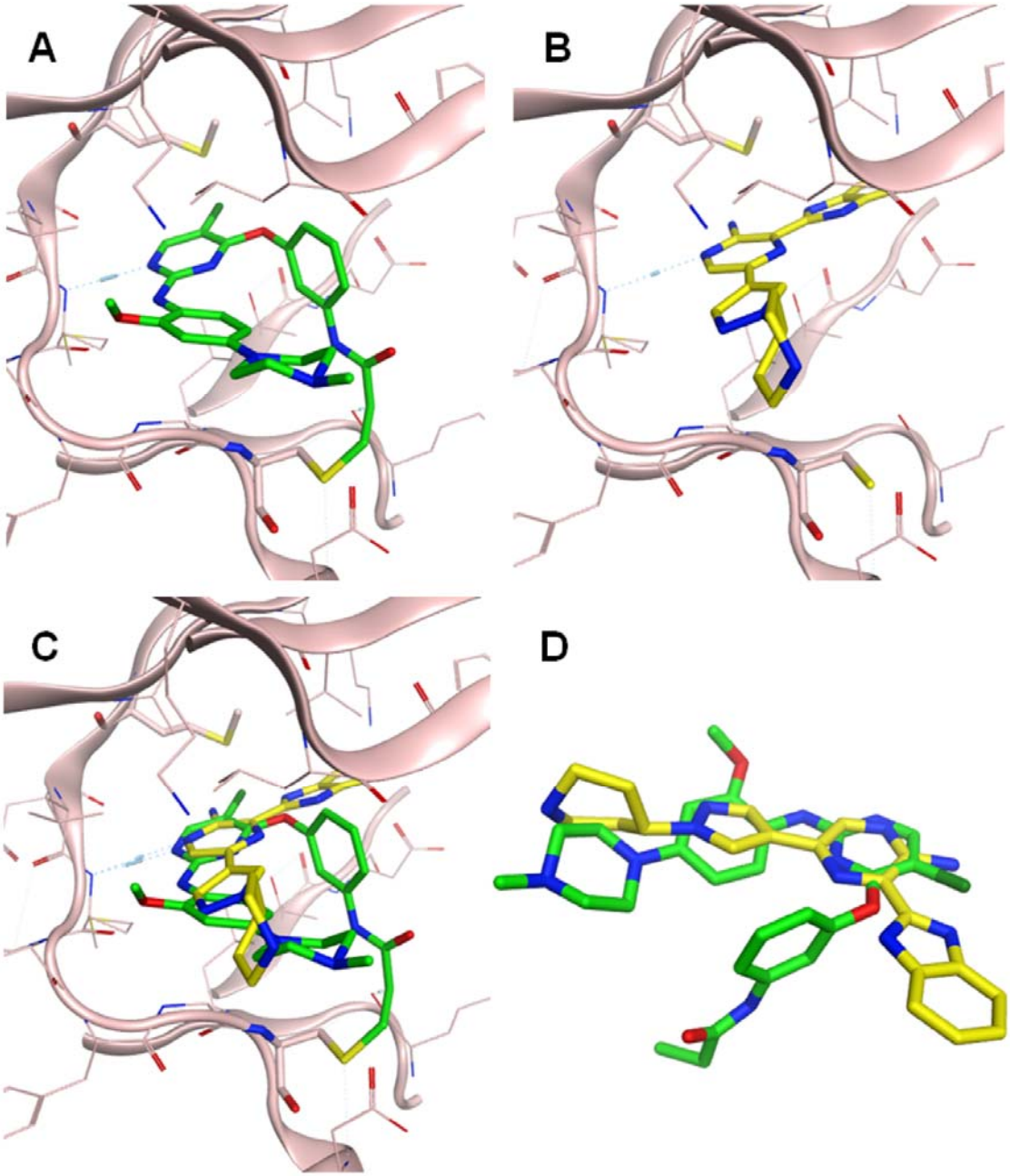

Figure S2. (A) Structure of WZ4002 (green) bound to EGFR T790M (PDB ID 3IKA). (B) Proposed position of aminopyrazine scaffold (yellow) in EGFR T790M ATP-binding site, based on unpublished crystal structures with other kinases. (C) Overlay of WZ4002 and aminopyrazine scaffold in ATP binding site. (D) Side view of overlay in absence of protein.

Procedures for the Synthesis of Compound 5:

General Considerations: All reagents and solvents used were purchased from commercial sources and were used without further purification. ^{1}H NMR and ^{13}C NMR spectra were obtained using a Bruker 300 MHz or 400 MHz spectrometer at temperatures ranging from 23 °C to 100 °C; chemical shifts are expressed in parts per million (ppm, δ units) and are referenced to the residual protons in the deuterated solvent used. Coupling constants are given in units of hertz (Hz). Splitting patterns describe apparent multiplicities and are designated as s (singlet), d (doublet), t (triplet), q (quartet), m (multiplet), and br s (broad singlet). Liquid chromatography - mass spectrometry (LC-MS) analyses were performed with an Agilent 1100 equipped with Waters columns (Atlantis T3, 2.1x50 mm, 3 μm; or Atlantis dC18, 2.1 x 50 mm, 5 μm) eluted with a gradient mixture of water and acetonitrile with either formic acid or ammonium acetate added as a modifier. High resolution mass spectrometry (HRMS) was run on a Bruker MicrOTOF-Q II, and samples were analyzed by electrospray positive ionization with external calibration. Reverse-phase chromatography was performed on a Gilson system using an Atlantis Prep T3 OBD reverse-phase HPLC column (19 mm x 100 mm) in water/MeCN with 0.1% TFA as mobile phase. Thin layer chromatography was performed using EMD silica gel 60 F_{254} plates, which were visualized using either UV light or a stain prepared by dissolving 2 g $KMnO_4$ and 12 g Na_2CO_3 in 200 mL H_2O. Column chromatography was performed using SiliCycle Silia*Sep* preloaded silica gel cartridges on Teledyne ISCO CombiFlash Companion automated purification systems. Unless otherwise indicated, all final compounds were purified to ≥ 95% purity as assessed by analytical HPLC using an Agilent 1100 equipped with Waters columns (Atlantis T3, 2.1x50 mm, 3 μm; or Atlantis dC18, 2.1 x 50 mm, 5 μm) eluted for > 10 minutes with a gradient mixture of water and acetonitrile with either formic acid or ammonium acetate added as a modifier, monitored at wavelengths of 220, 254, and 280 nm.

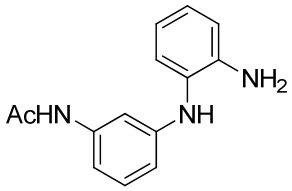

***N*-(3-(2-Aminophenylamino)phenyl)acetamide (6):** A 500 mL roundbottom flask was charged with N-(3-aminophenyl)acetamide (8.25 g, 54.9 mmol) and DMF (40 mL). 1-Fluoro-2-nitrobenzene (5.30 mL, 50.3 mmol) and 4-methylmorpholine (8.30 mL, 75.5 mmol) were added followed by additional DMF (10 mL), and the resulting solution was heated in a 125 °C oil bath. After heating for 72 hours, the dark red mixture was allowed to cool to room temperature. Water (200 mL) was added, causing a solid material to precipitate from the mixture. The suspension was allowed to stir at room temperature for ~10 minutes before being suction filtered. The filter cake was washed with water and was dried in air to give *N*-(3-(2-nitrophenylamino)phenyl)acetamide as a bright orange solid (9.77 g, 72%). ^{1}H NMR (400 MHz, DMSO-d_6) δ ppm 2.04 (s, 3H), 6.85 - 6.92 (m, 1H), 6.95 - 7.00 (m, 1H), 7.21 - 7.26 (m, 1H), 7.27 - 7.38 (m, 2H), 7.46 - 7.58 (m, 1H), 7.62 - 7.66 (m, 1H), 8.08 - 8.13 (m, 1H), 9.30 (s, 1H), 10.00 (s, 1H). LC-MS (M+H) 272.

A 250 mL roundbottom flask was charged with *N*-(3-(2-nitrophenylamino)phenyl)acetamide (4.32 g, 15.9 mmol) and ammonium chloride (8.75 g, 164 mmol). MeOH (100 mL) and water (25 mL) were added, and the mixture was placed in a room temperature water bath. Zinc dust (6.61 g, 101 mmol) was added in portions (CAUTION: the initial reaction was exothermic), and the mixture was allowed to stir at room temperature for a few minutes until the exotherm had subsided. The mixture was then heated in a 60 °C oil bath overnight. The reaction mixture was allowed to cool and was suction filtered, and the reaction flask and filter cake were washed well with MeOH. The combined filtrates were concentrated under reduced pressure, and the residue was partitioned between EtOAc and water. The aqueous layer was

extracted with EtOAc, and the combined organics were washed with water and were concentrated under reduced pressure to give the title compound as a tan solid (3.39 g, 88%). ^{1}H NMR (400 MHz, DMSO-d_6) δ ppm 1.98 (s, 3H), 4.72 (s, 2H), 6.37 - 6.43 (m, 1H), 6.49 - 6.58 (m, 1H), 6.70 - 6.75 (m, 1H), 6.79 - 6.86 (m, 1H), 6.89 - 6.95 (m, 1H), 6.95 - 7.04 (m, 3H), 7.09 (s, 1H), 9.68 (s, 1H). LC-MS (M+H) 242.

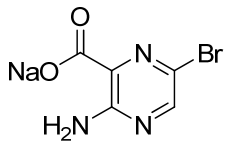

3-Amino-6-bromopyrazine-2-carboxylic acid sodium salt hydrate (7): A 500 mL roundbottom flask was charged with methyl 3-amino-6-bromopyrazine-2-carboxylate (26.90 g, 115.9 mmol) and sodium hydroxide (6.86 g, 171.5 mmol). Water (250 mL) was added, and the resulting suspension was heated to reflux. After heating overnight, the reaction was allowed to thoroughly cool to room temperature. The mixture was suction filtered, and the filter cake was washed with water and was dried in air to give the title compound as a pale orange crystalline solid (30.0 g, quantitative). ^{1}H NMR (400 MHz, DMSO-d_6) δ ppm 7.98 (s). LC-MS (M+H) 218, 220.

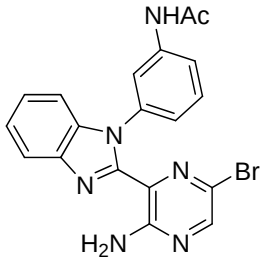

***N*-(3-(2-(3-Amino-6-bromopyrazin-2-yl)-1*H*-benzo[d]imidazol-1-yl)phenyl)acetamide (8):** A 250 mL roundbottom flask was charged with *N*-(3-(2-aminophenylamino)phenyl)acetamide (**6**; 2.21 g, 9.16 mmol) and 3-amino-6-bromopyrazine-

2-carboxylic acid sodium salt hydrate (**7**; 2.59 g, 10.0 mmol). Anhydrous DMF (15 mL) was added, and the resulting heterogeneous mixture was treated with HATU (4.29 g, 11.3 mmol). Additional DMF (5 mL) was added and the mixture was allowed to stir at room temperature for 2 hours. The reaction was then partitioned between EtOAc and water. The aqueous layer was extracted with EtOAc (2x), and the combined organics were washed with water and were concentrated under reduced pressure to give the intermediate *N*-(2-(3-acetamidophenylamino)phenyl)-3-amino-6-bromopyrazine-2-carboxamide as a yellow-colored solid. This material was treated with glacial HOAc (25 mL), and the resulting yellow suspension was heated in a 110 °C oil bath. After heating overnight (18 hours), the oil bath temperature was increased to 120 °C and heating was continued for an additional 24 hours. The reaction was allowed to cool to room temperature and was concentrated under reduced pressure. The crude material was purified by silica gel chromatography (gradient elution; R_f in 50:50 hexanes:EtOAc = 0.40) to give the title compound as a yellow solid (2.66 g, 69%). ^{1}H NMR (400 MHz, DMSO-d_6) δ ppm 2.05 (s, 3H), 7.01 - 7.07 (m, 1H), 7.13 - 7.19 (m, 1H), 7.28 - 7.42 (m, 2H), 7.42 - 7.52 (m, 1H), 7.60 - 7.72 (m, 2H), 7.86 - 7.91 (m, 1H), 8.13 (s, 1H), 8.17 (br. s., 2H), 10.13 (s, 1H). LC-MS (M+H) 423, 425.

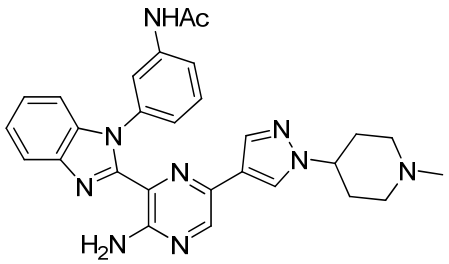

***N*-(3-(2-(3-Amino-6-(1-(1-methylpiperidin-4-yl)-1H-pyrazol-4-yl)pyrazin-2-yl)-1*H*-benzo[d]imidazol-1-yl)phenyl)acetamide (9):** A 250 mL roundbottom flask was charged with *N*-(3-(2-(3-amino-6-bromopyrazin-2-yl)-1*H*-benzo[d]imidazol-1-yl)phenyl)acetamide (**8**; 1.38 g, 3.26 mmol), *tert*-butyl 4-(4-(4,4,5,5-tetramethyl-1,3,2-dioxaborolan-2-yl)-1*H*-

pyrazol-1-yl)piperidine-1-carboxylate[1] (1.53 g, 4.06 mmol), $Pd_2(dba)_3$ (67.2 mg, 4.5 mol %), dicyclohexyl(2',6'-dimethoxybiphenyl-2-yl)phosphine (SPhos; 72.0 mg, 5.4 mol %), and Cs_2CO_3 (3.28 g, 10.1 mmol). The flask was evacuated and backfilled with N_2 (3x), and then anhydrous dioxane (15.0 mL) was added. The mixture was allowed to stir at room temperature for 10 minutes before water (3.0 mL) was added. The resulting mixture was placed in an oil bath preheated to 100 °C. After heating overnight, the reaction was allowed to cool to room temperature. The mixture was partitioned between EtOAc and water, and the aqueous layer was further extracted with EtOAc. The combined organics were concentrated under reduced pressure, and the crude material was purified by silica gel chromatography (gradient elution; R_f in EtOAc = 0.48) to give the *tert*-butyl 4-(4-(6-(1-(3-acetamidophenyl)-1*H*-benzo[d]imidazol-2-yl)-5-aminopyrazin-2-yl)-1*H*-pyrazol-1-yl)piperidine-1-carboxylate as an orange-yellow solid (1.75 g, 90%). ^{1}H NMR (400 MHz, DMSO-d_6) δ ppm 1.44 (s, 9H), 1.60 - 1.75 (m, 2H), 1.92 - 2.00 (m, 2H), 2.05 (s, 3H), 2.85 - 3.03 (m, 2H), 4.01 - 4.11 (m, 2H), 4.17 - 4.27 (m, 1H), 7.07 - 7.11 (m, 2H), 7.28 - 7.40 (m, 4H), 7.50 - 7.54 (m, 1H), 7.63 - 7.72 (m, 1H), 7.79 - 7.83 (m, 1H), 7.86 - 7.88 (m, 1H), 7.99 (br. s., 2H), 8.38 (s, 1H), 10.20 (s, 1H). LC-MS (M+H) 594. A 500 mL roundbottom flask containing this material (1.40 g, 2.36 mmol) was treated with CH_2Cl_2 (10.0 mL) and trifluoroacetic acid (5.0 mL, 64.9 mmol), and the resulting solution was allowed to stir at room temperature. After 1.5 hours, the reaction was concentrated under reduced pressure. The residue was treated with EtOAc and half-saturated $NaHCO_3$, and the biphasic mixture was allowed to stir at room temperature, eventually becoming heterogeneous. After stirring overnight, the mixture was suction filtered. The filter cake was washed with both water and EtOAc and was then dried in air to give *N*-(3-(2-(3-amino-6-(1-(piperidin-4-yl)-1*H*-pyrazol-4-yl)pyrazin-2-yl)-1*H*-benzo[d]imidazol-1-yl)phenyl)acetamide as a yellow solid (1.20 g, quantitative). ^{1}H NMR (400 MHz, DMSO-d_6) δ ppm 1.62 - 1.75 (m, 2H), 1.86 - 1.95 (m, 2H), 2.06 (s, 3H), 2.59 -

2.72 (m, 2H), 3.05 - 3.15 (m, 2H), 4.04 - 4.16 (m, 1H), 7.03 - 7.11 (m, 2H), 7.13 (s, 1H), 7.25 - 7.40 (m, 2H), 7.42 (s, 1H), 7.50 - 7.57 (m, 1H), 7.70 - 7.77 (m, 1H), 7.79 - 7.91 (m, 2H), 8.00 (br. s., 2H), 8.39 (s, 1H), 10.31 (br. s., 1H). LC-MS (M+H) 494. A 100 mL roundbottom flask was charged with this material (443 mg, 0.90 mmol). MeOH (10 mL) and formaldehyde (37% aqueous solution; 300 μL, 4.0 mmol) were added, and the resulting suspension was treated with sodium cyanoborohydride (159 mg, 2.53 mmol). After stirring at room temperature for 2 hours, the yellow suspension was diluted with water (25 mL). The mixture was allowed to stir for ~30 minutes before being suction filtered. The filter cake was washed with water and was dried in air to give the title compound as a bright yellow solid (427 mg, 93%). ^{1}H NMR (400 MHz, DMSO-d_6) δ ppm 1.76 - 1.97 (m, 4H), 1.98 - 2.10 (m, 2H), 2.05 (s, 3H), 2.23 (s, 3H), 2.83 - 2.91 (m, 2H), 3.91 - 4.03 (m, 1H), 7.04 - 7.11 (m, 2H), 7.24 (s, 1H), 7.27 - 7.41 (m, 3H), 7.50 - 7.54 (m, 1H), 7.69 - 7.72 (m, 1H), 7.78 - 7.80 (m, 1H), 7.86 - 7.88 (m, 1H), 7.98 (br. s., 2H), 8.38 (s, 1H), 10.22 (s, 1 H). LC-MS (M+H) 508.

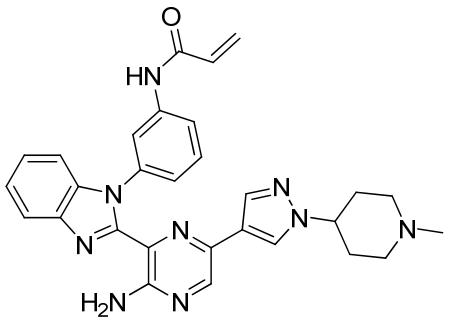

***N*-(3-(2-(3-Amino-6-(1-(1-methylpiperidin-4-yl)-1*H*-pyrazol-4-yl)pyrazin-2-yl)-1*H*-benzo[d]imidazol-1-yl)phenyl)acrylamide (5):** A 100 mL roundbottom flask was charged with *N*-(3-(2-(3-amino-6-(1-(1-methylpiperidin-4-yl)-1*H*-pyrazol-4-yl)pyrazin-2-yl)-1*H*-benzo[d]imidazol-1-yl)phenyl)acetamide (**9**; 370 mg, 0.73 mmol). Water (5.0 mL) and concentrated HCl (1.0 mL, 12 mmol) were added, and the mixture was heated in a 100 °C oil bath, resulting in an orange-colored solution. After heating overnight, the reaction was

allowed to cool to room temperature and was treated with EtOAc (~5 mL). A solution of NaOH (838 mg, 21 mmol) in water (10 mL) was added, forming a thick yellow suspension. The mixture was allowed to stir for a few minutes before being suction-filtered. The filter cake was washed with water and was dried in air to give 3-(1-(3-aminophenyl)-1*H*-benzo[d]imidazol-2-yl)-5-(1-(1-methylpiperidin-4-yl)-1*H*-pyrazol-4-yl)pyrazin-2-amine as a yellow solid (263 mg, 77%). ^{1}H NMR (400 MHz, DMSO-d_6) δ ppm 1.82 - 2.01 (m, 4H), 2.01 - 2.13 (m, 2H), 2.23 (s, 3H), 2.83 - 2.93 (m, 2H), 3.93 - 4.07 (m, 1H), 5.39 (s, 2H), 6.45 - 6.53 (m, 1H), 6.53 - 6.58 (m, 1H), 6.72 - 6.81 (m, 1H), 7.06 - 7.14 (m, 1H), 7.20 - 7.28 (m, 1H), 7.28 - 7.37 (m, 2H), 7.40 (s, 1H), 7.45 (s, 1H), 7.79 - 7.87 (m, 1H), 7.96 (br. s., 2H), 8.37 (s, 1H). LC-MS (M+H) 466. A 250 mL roundbottom flask containing this compound (245 mg, 0.53 mmol) was treated with EtOAc (5 mL) and DMF (1 mL). The resulting solution was treated with 4-methylmorpholine (170 µL, 1.55 mmol) followed by acryloyl chloride (70 µL, 0.86 mmol). A gummy solid quickly precipitated, and additional DMF (1 mL) was added to improve solubility. The reaction was sonicated to break up the gummy precipitate, and the resulting suspension was allowed to stir at room temperature. After 90 minutes, the reaction mixture was partitioned between EtOAc and water. The aqueous layer was extracted with EtOAc (2x), and the combined organics were washed with water and concentrated under reduced pressure. The resulting yellow oil was dissolved in MeOH (3 mL), and on standing overnight a yellow solid had crystallized from the solution. The mixture was stored in a freezer for several hours and was then suction-filtered. The yellow filter cake was washed with a minimum of cold MeOH and was dried in air to give the title compound as a yellow solid (101 mg, 37%). ^{1}H NMR (400 MHz, DMSO-d_6) δ ppm 1.76 - 1.95 (m, 4H), 1.98 - 2.10 (m, 2H), 2.21 (s, 3H), 2.78 - 2.89 (m, 2H), 3.88 - 4.00 (m, 1H), 5.75 - 5.81 (m, 1H), 6.21 - 6.30 (m, 1H), 6.37 - 6.48 (m, 1H), 7.03 - 7.15 (m, 2H), 7.23 (s, 1H), 7.28 - 7.45 (m, 3H), 7.54 - 7.60 (m, 1H), 7.78 - 7.83 (m, 1H), 7.84 - 7.94 (m, 2H), 7.99 (br. s.,

2H), 8.39 (s, 1H), 10.43 (s, 1H). ^{13}C NMR (101 MHz, DMSO-d_6) δ ppm 31.9, 45.7, 53.9, 58.1, 110.5, 117.7, 118.6, 119.3, 122.3, 123.1, 124.0, 124.2, 124.4, 127.3, 130.0, 131.6, 134.3, 135.1, 137.0, 139.3, 139.7, 140.2, 141.1, 148.4, 152.3, 163.4. HRMS-ESI (M+H): calcd for $C_{29}H_{30}N_9O_1$, 520.2568; found, 520.2566.

Characterization data for other reported compounds:

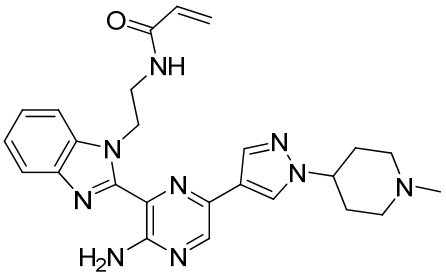

***N*-(2-(2-(3-amino-6-(1-(1-methylpiperidin-4-yl)-1*H*-pyrazol-4-yl)pyrazin-2-yl)-1*H*-benzo[d]imidazol-1-yl)ethyl)acrylamide (3):** ^{1}H NMR (400 MHz, DMSO-d_6) δ ppm 1.96 - 2.11 (m, 6H), 2.22 (s, 3H), 2.83 - 2.92 (m, 2H), 3.73 (q, *J* = 6.1 Hz, 2H), 4.19 (br. s., 1H), 4.96 - 5.07 (m, 2H), 5.46 - 5.56 (m, 1H), 5.95 - 6.08 (m, 2H), 7.22 - 7.40 (m, 2H), 7.62 (d, *J* = 8.1 Hz, 1H), 7.76 (d, *J* = 7.3 Hz, 1H), 7.99 (s, 1H), 8.24 - 8.35 (m, 2H), 8.52 (s, 1H). LC-MS (M+H) 472.

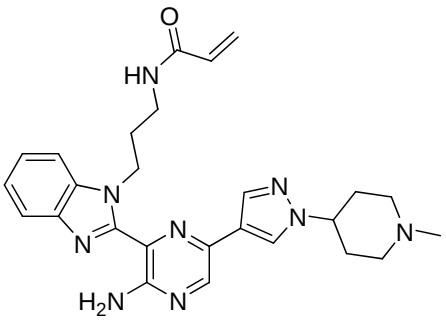

N-(3-(2-(3-amino-6-(1-(1-methylpiperidin-4-yl)-1H-pyrazol-4-yl)pyrazin-2-yl)-1H-benzo[d]imidazol-1-yl)propyl)acrylamide (4):. ^{1}H NMR (400 MHz, DMSO-d_6) δ ppm 1.93 - 2.13 (m, 8H), 2.21 (s, 3H), 2.81 - 2.92 (m, 2H), 3.16 - 3.25 (m, 2H), 4.19 (br. s., 1H), 4.95 (t, *J* = 7.2 Hz, 2H), 5.55 (dd, *J* = 2.4, 10.0 Hz, 1H), 6.03 (dd, *J* = 2.4, 17.1 Hz, 1H), 6.15 (dd, *J* = 10.0, 17.1 Hz, 1H), 7.28 - 7.42 (m, 2H), 7.71 (d, *J* = 8.4 Hz, 1H), 7.78 (d, *J* = 7.8 Hz, 1H), 7.99 (s, 1H), 8.14 (t, *J* = 5.1 Hz, 1H), 8.31 (s, 1H), 8.52 (s, 1H). LC-MS (M+H) 486.

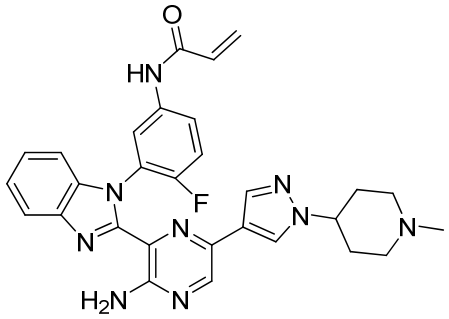

***N*-(3-(2-(3-Amino-6-(1-(1-methylpiperidin-4-yl)-1*H*-pyrazol-4-yl)pyrazin-2-yl)-1*H*-benzo[d]imidazol-1-yl)-4-fluorophenyl)acrylamide (10):** ^{1}H NMR (400 MHz, DMSO-d_6) δ ppm 1.97 - 2.14 (m, 2H), 2.14 - 2.27 (m, 2H), 2.79 - 2.90 (m, 3H), 3.08 - 3.25 (m, 2H), 3.54 - 3.62 (m, 2H), 4.30 - 4.46 (m, 1H), 5.81 (dd, *J* = 1.8, 10.1 Hz, 1H), 6.29 (dd, *J* = 1.8, 16.9 Hz, 1H), 6.44 (dd, *J* = 10.1, 16.9 Hz, 1H), 7.16 (d, *J* = 7.3 Hz, 1H), 7.30 - 7.46 (m, 4H), 7.47 - 7.58 (m, 1H), 7.86 - 7.94 (m, 2H), 7.95 - 8.17 (m, 3H), 8.41 - 8.50 (m, 1H), 9.53 (br. s., 1H), 10.53 (s, 1H). LC-MS (M+H) 538.

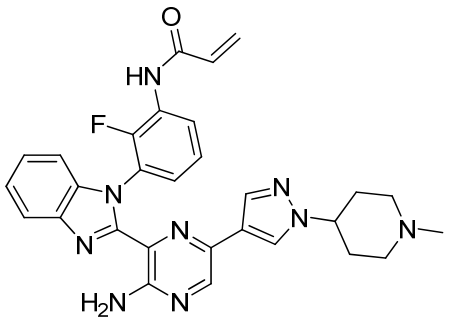

***N*-(3-(2-(3-Amino-6-(1-(1-methylpiperidin-4-yl)-1*H*-pyrazol-4-yl)pyrazin-2-yl)-1*H*-benzo[d]imidazol-1-yl)-2-fluorophenyl)acrylamide (11):** ^{1}H NMR (400 MHz, DMSO-d_6) δ ppm 1.98 - 2.24 (m, 4H), 2.80 - 2.90 (m, 3H), 3.10 - 3.24 (m, 2H), 3.39 - 3.47 (m, 2H), 4.26 - 4.42 (m, 1H), 5.79 (d, *J* = 10.1 Hz, 1H), 6.31 (dd, *J* = 1.8, 17.2 Hz, 1H), 6.59 (dd, *J* = 9.9, 17.2 Hz, 1H), 7.05 - 7.17 (m, 2H), 7.33 - 7.42 (m, 2H), 7.42 - 7.53 (m, 3H), 7.91 (d, *J* = 7.6 Hz, 1H), 8.11 (s, 2H), 8.38 - 8.50 (m, 2H), 9.40 (br. s., 1H), 10.13 (s, 1H). LC-MS (M+H) 538.

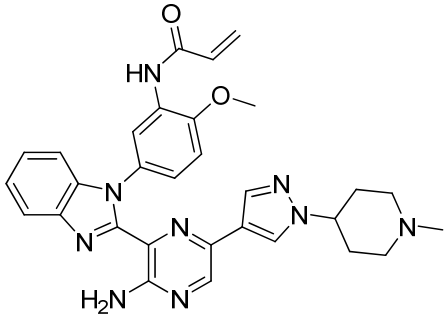

***N*-(5-(2-(3-Amino-6-(1-(1-methylpiperidin-4-yl)-1*H*-pyrazol-4-yl)pyrazin-2-yl)-1*H*-benzo[d]imidazol-1-yl)-2-methoxyphenyl)acrylamide (12):** ^{1}H NMR (400 MHz, DMSO-d_6) δ ppm 2.01 - 2.16 (m, 2H), 2.16 - 2.26 (m, 2H), 2.80 - 2.88 (m, 3H), 3.05 - 3.20 (m, 2H), 3.59 (d, *J* = 12.4 Hz, 2H), 3.95 - 4.01 (m, 3H), 4.23 - 4.36 (m, 1H), 5.73 (d, *J* = 11.6 Hz, 1H), 6.19 (dd, *J* = 1.9, 17.1 Hz, 1H), 6.76 (dd, *J* = 10.1, 16.7 Hz, 1H), 7.11 (d, *J* = 7.3 Hz, 1H), 7.16 (dd, *J* = 2.5, 8.6 Hz, 1H), 7.24 - 7.29 (m, 2H), 7.30 - 7.39 (m, 2H), 7.60 (s, 1H), 7.87 (d, *J* = 7.1 Hz, 1H), 8.00 (br. s., 2H), 8.25 (s, 1H), 8.37 - 8.45 (m, 1H), 9.43 (br. s., 1H), 9.60 - 9.71 (m, 1H). LC-MS (M+H) 550.

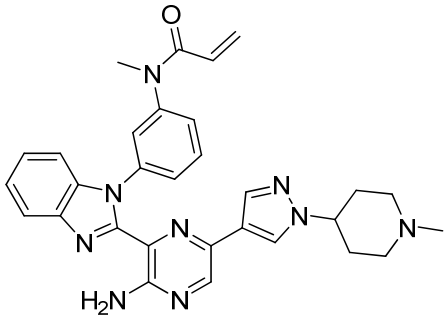

***N*-(3-(2-(3-Amino-6-(1-(1-methylpiperidin-4-yl)-1*H*-pyrazol-4-yl)pyrazin-2-yl)-1*H*-benzo[d]imidazol-1-yl)phenyl)-*N*-methylacrylamide (13):** ^{1}H NMR (400 MHz, DMSO-d_6, 100 °C) δ ppm 1.84 - 2.02 (m, 4H), 2.05 - 2.17 (m, 2H), 2.25 (s, 3H), 2.81 - 2.90 (m, 2H), 3.19 (s, 3H), 3.96 - 4.08 (m, 1H), 5.24 - 5.32 (m, 1H), 5.95 - 6.15 (m, 2H), 7.12 - 7.19 (m, 1H), 7.23 - 7.29 (m, 2H), 7.29 - 7.40 (m, 2H), 7.42 - 7.51 (m, 2H), 7.52 - 7.57 (m, 1H), 7.65 (br. s., 2H), 7.70 - 7.79 (m, 1H), 7.80 - 7.89 (m, 1H), 8.36 (s, 1H). LC-MS (M+H) 534.

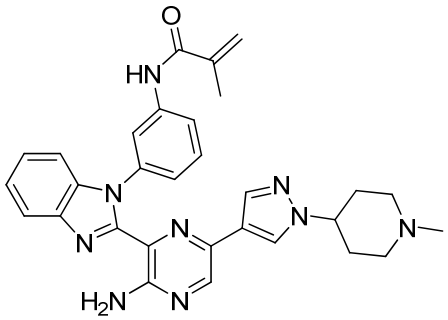

***N*-(3-(2-(3-Amino-6-(1-(1-methylpiperidin-4-yl)-1*H*-pyrazol-4-yl)pyrazin-2-yl)-1*H*-benzo[d]imidazol-1-yl)phenyl)methacrylamide (14):** ^{1}H NMR (400 MHz, DMSO-d_6) δ ppm 1.77 - 1.99 (m, 7H), 2.02 - 2.14 (m, 2H), 2.17 - 2.28 (m, 3H), 2.81 - 2.92 (m, 2H), 3.91 - 4.03 (m, 1H), 5.53 - 5.56 (m, 1H) 5.81 - 5.86 (m, 1H), 7.06 - 7.14 (m, 2H), 7.19 (s, 1H), 7.29 - 7.40 (m, 2H), 7.42 - 7.45 (m, 1H), 7.49 - 7.57 (m, 1H), 7.79 - 7.84 (m, 1H), 7.85 - 7.90 (m, 1H), 7.93 - 8.10 (m, 3H), 8.39 (s, 1H), 10.04 (s, 1H). LC-MS (M+H) 534.

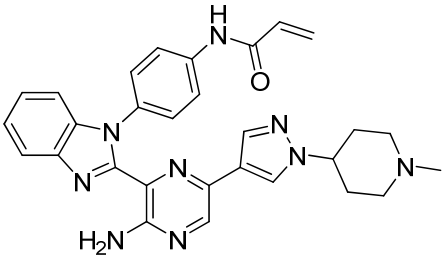

***N*-(4-(2-(3-Amino-6-(1-(1-methylpiperidin-4-yl)-1*H*-pyrazol-4-yl)pyrazin-2-yl)-1*H*-benzo[d]imidazol-1-yl)phenyl)acrylamide (15):** ^{1}H NMR (400 MHz, DMSO-d_6) δ ppm 2.00 - 2.25 (m, 4H), 2.64 - 2.80 (m, 3H), 2.92 - 3.19 (m, 2H), 3.36 - 3.55 (m, 2H), 4.20 - 4.37 (m, 1H), 5.80 - 5.90 (m, 1H), 6.31 - 6.41 (m, 1H), 6.56 - 6.70 (m, 1H), 7.05 - 7.13 (m, 1H), 7.16 - 7.25 (m, 1H), 7.28 - 7.39 (m, 2H), 7.40 - 7.47 (m, 2H), 7.50 - 7.57 (m, 1H), 7.83 - 7.91 (m, 1H), 7.91 - 8.12 (m, 3H), 8.41 (s, 1H), 10.19 - 10.37 (m, 1H), 10.69 - 10.82 (m, 1H). LC-MS (M+H) 520.

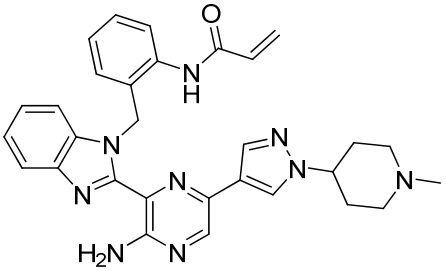

***N*-(2-((2-(3-Amino-6-(1-(1-methylpiperidin-4-yl)-1*H*-pyrazol-4-yl)pyrazin-2-yl)-1*H*-benzo[d]imidazol-1-yl)methyl)phenyl)acrylamide (16):** ^{1}H NMR (400 MHz, DMSO-d_6) δ ppm 1.74 - 1.89 (m, 4H), 1.94 - 2.05 (m, 2H), 2.19 (s, 3H), 2.80 (d, J = 11.3 Hz, 2H), 3.88 - 4.01 (m, 1H), 5.78 - 5.84 (m, 1H), 6.07 (s, 2H), 6.32 (dd, J = 1.8, 17.1 Hz, 1H), 6.53 - 6.63 (m, 2H), 7.02 (t, J = 7.5 Hz, 1H), 7.25 - 7.35 (m, 4H), 7.56 (d, J = 8.0 Hz, 1H), 7.59 - 7.64 (m, 2H), 7.79 - 7.87 (m, 1H), 8.07 (br. s., 2H), 8.49 (s, 1H), 10.05 (s, 1H). LC-MS (M+H) 534.

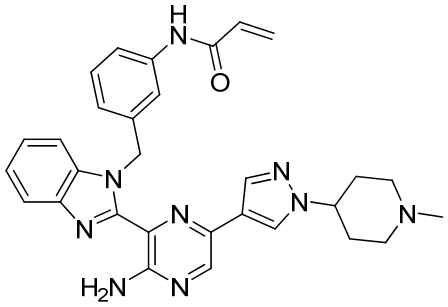

***N*-(3-((2-(3-Amino-6-(1-(1-methylpiperidin-4-yl)-1*H*-pyrazol-4-yl)pyrazin-2-yl)-1*H*-benzo[d]imidazol-1-yl)methyl)phenyl)acrylamide (17):** ^{1}H NMR (400 MHz, DMSO-d_6) δ ppm 1.74 - 1.90 (m, 4H), 1.95 - 2.07 (m, 2H), 2.19 (s, 3H), 2.80 (d, *J* = 11.1 Hz, 2H), 3.86 - 3.99 (m, 1H), 5.65 - 5.73 (m, 1H), 6.09 - 6.23 (m, 3H), 6.28 - 6.39 (m, 1H), 6.88 (d, *J* = 7.8 Hz, 1H), 7.25 - 7.36 (m, 3H), 7.42 (s, 1H), 7.45 - 7.49 (m, 1H), 7.55 (s, 1H), 7.63 (s, 1H), 7.69 (d, *J* = 7.3 Hz, 1H), 7.80 - 7.88 (m, 1H), 8.06 (br. s., 2H), 8.48 (s, 1H), 10.06 (s, 1H). LC-MS (M+H) 534.

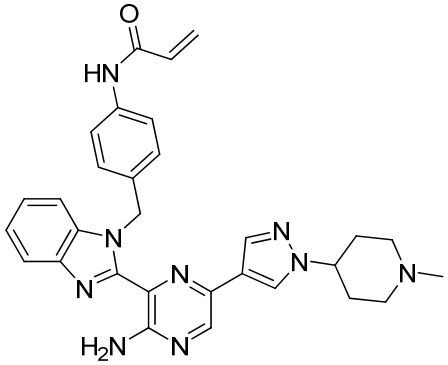

N-(4-((2-(3-Amino-6-(1-(1-methylpiperidin-4-yl)-1*H*-pyrazol-4-yl)pyrazin-2-yl)-1*H*-benzo[d]imidazol-1-yl)methyl)phenyl)acrylamide (18): ^{1}H NMR (400 MHz, DMSO-d_6) δ ppm 1.99 - 2.25 (m, 4H), 2.77 - 2.88 (m, 3H), 3.04 - 3.20 (m, 2H), 3.56 (d, *J* = 11.9 Hz, 2H), 4.34 (ddd, *J* = 4.3, 11.5, 15.5 Hz, 1H), 5.74 (dd, *J* = 2.0, 10.1 Hz, 1H), 6.15 (s, 2H), 6.24 (dd, *J* = 2.2, 17.1 Hz, 1H), 6.40 (ddd, *J* = 3.5, 10.1, 16.9 Hz, 1H), 7.13 (d, *J* = 8.6 Hz, 2H), 7.30 - 7.36 (m, 2H), 7.51 - 7.57 (m, 1H), 7.59 (d, *J* = 8.6 Hz, 2H), 7.68 - 7.75 (m, 2H), 7.78 - 7.86 (m, 1H), 8.45 - 8.58 (m, 1H), 9.43 (br. s., 1H), 10.15 (s, 1H). LC-MS (M+H) 534.

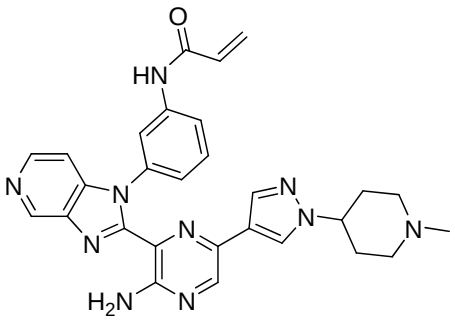

***N*-(3-(2-(3-Amino-6-(1-(1-methylpiperidin-4-yl)-1*H*-pyrazol-4-yl)pyrazin-2-yl)-1*H*-imidazo[4,5-c]pyridin-1-yl)phenyl)acrylamide (19):** ^{1}H NMR (400 MHz, DMSO-d_6) δ ppm 1.76 - 1.94 (m, 4H), 1.97 - 2.09 (m, 2H), 2.21 (s, 3H), 2.78 - 2.90 (m, 2H), 3.89 - 4.00 (m, 1H), 5.73 - 5.83 (m, 1H), 6.22 - 6.33 (m, 1H), 6.37 - 6.50 (m, 1H), 7.13 - 7.20 (m, 2H), 7.26 (s, 1H), 7.38 (s, 1H), 7.53 - 7.62 (m, 1H), 7.81 - 7.87 (m, 1H), 7.89 - 7.95 (m, 1H), 7.97 (br. s., 2H), 8.38 - 8.43 (m, 1H), 8.45 (s, 1H), 9.15 - 9.20 (m, 1H), 10.48 (s, 1H). LC-MS (M+H) 521.

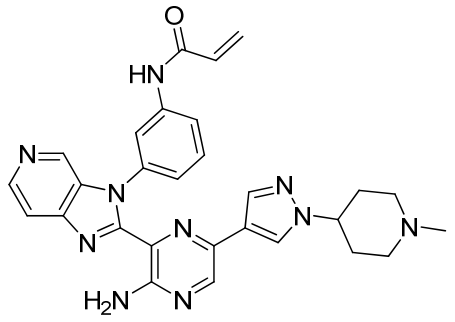

***N*-(3-(2-(3-Amino-6-(1-(1-methylpiperidin-4-yl)-1*H*-pyrazol-4-yl)pyrazin-2-yl)-3*H*-imidazo[4,5-c]pyridin-3-yl)phenyl)acrylamide (20):** ^{1}H NMR (400 MHz, DMSO-d_6) δ ppm 1.98 - 2.13 (m, 2H), 2.19 (d, *J* = 10.9 Hz, 2H), 2.75 - 2.90 (m, 3H), 3.07 - 3.24 (m, 2H), 3.55 - 3.62 (m, 2H), 4.27 - 4.40 (m, 1H), 5.74 - 5.85 (m, 1H), 6.27 (dd, *J* = 1.9, 17.1 Hz, 1H), 6.44 (dd, *J* = 10.0, 17.1 Hz, 1H), 7.27 - 7.40 (m, 3H), 7.64 (t, *J* = 8.1 Hz, 1H), 7.84 (s, 1H),

8.03 (d, *J* = 7.3 Hz, 1H), 8.07 - 8.19 (m, 3H), 8.54 - 8.57 (m, 1H), 8.59 (d, *J* = 6.1 Hz, 1H), 8.70 (s, 1H), 9.49 (br. s., 1H), 10.45 - 10.55 (m, 1H). LC-MS (M+H) 521.

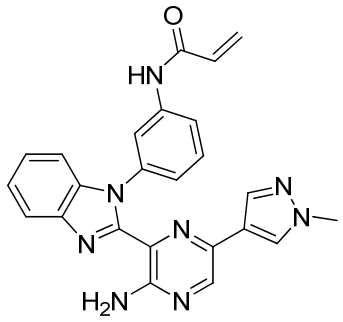

***N*-(3-(2-(3-Amino-6-(1-methyl-1*H*-pyrazol-4-yl)pyrazin-2-yl)-1*H*-benzo[d]imidazol-1-yl)phenyl)acrylamide (21):** ^{1}H NMR (400 MHz, DMSO-d_6) δ ppm 3.74 (s, 3H), 5.73 - 5.81 (m, 1H), 6.20 - 6.30 (m, 1H), 6.36 - 6.48 (m, 1H), 7.07 - 7.16 (m, 2H), 7.22 (s, 1 H) 7.26 - 7.41 (m, 3H), 7.53 - 7.61 (m, 1H), 7.79 - 7.83 (m, 1H), 7.83 - 7.90 (m, 2H), 7.98 (br. s., 2H), 8.36 (s, 1H), 10.42 (s, 1H). LC-MS (M+H) 437.

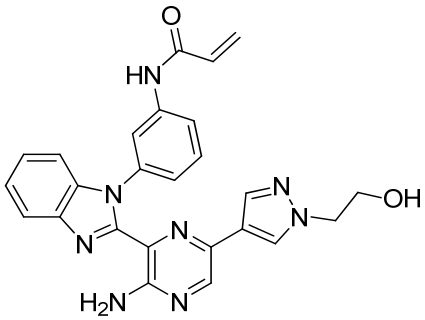

***N*-(3-(2-(3-amino-6-(1-(2-hydroxyethyl)-1*H*-pyrazol-4-yl)pyrazin-2-yl)-1*H*-benzo[d]imidazol-1-yl)phenyl)acrylamide (22):** ^{1}H NMR (400 MHz, DMSO-d_6) δ ppm 3.69 (t, *J*=5.5 Hz, 2H), 4.04 (t, *J*=5.5 Hz, 2H), 4.82 - 4.90 (m, 1H), 5.73 - 5.80 (m, 1H), 6.24 (dd, *J*=17.1, 2.0 Hz, 1H), 6.42 (dd, *J*=17.1, 10.0 Hz, 1H), 7.09 - 7.19 (m, 3H), 7.30 - 7.41 (m, 2H), 7.43 (s, 1H), 7.55 - 7.62 (m, 1H), 7.81 - 7.86 (m, 2H), 7.88 (d, *J*=7.3 Hz, 1H), 8.00 (br. s., 2H), 8.38 (s, 1H), 10.42 (s, 1H). LCMS (M+H) 467.

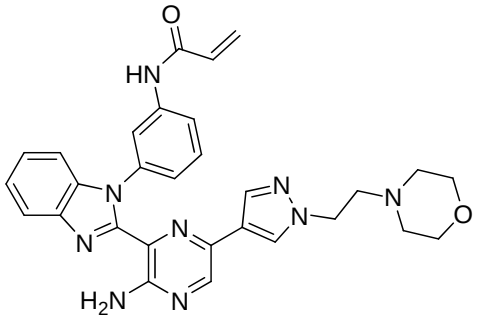

***N*-(3-(2-(3-Amino-6-(1-(2-morpholinoethyl)-1*H*-pyrazol-4-yl)pyrazin-2-yl)-1*H*-benzo[d]imidazol-1-yl)phenyl)acrylamide (23):** ^{1}H NMR (400 MHz, DMSO-d_6) δ ppm 2.35 - 2.42 (m, 4H), 2.65 (t, *J*=6.7 Hz, 2H), 3.49 - 3.58 (m, 4H), 4.11 (t, *J*=6.7 Hz, 2H), 5.75 - 5.82 (m, 1H), 6.26 (dd, *J*=17.0, 1.9 Hz, 1H), 6.43 (dd, *J*=17.0, 10.2 Hz, 1H), 7.09 - 7.16 (m, 2H), 7.26 (s, 1H), 7.30 (s, 1H), 7.33 - 7.43 (m, 2H), 7.57 (t, *J*=8.0 Hz, 1H), 7.79 (s, 1H), 7.85 - 7.95 (m, 2H), 8.01 (br. s., 1H), 8.38 (s, 1H), 10.43 (s, 1H). LC-MS (M+H) 536.

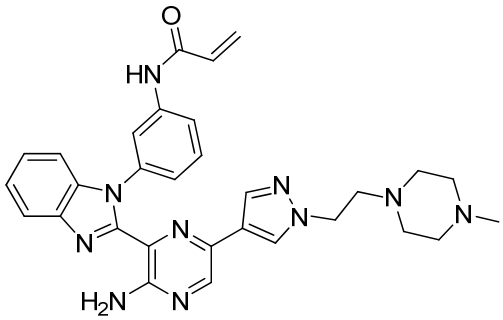

***N*-(3-(2-(3-Amino-6-(1-(2-(4-methylpiperazin-1-yl)ethyl)-1*H*-pyrazol-4-yl)pyrazin-2-yl)-1*H*-benzo[d]imidazol-1-yl)phenyl)acrylamide (24):** ^{1}H NMR (400 MHz, DMSO-d_6) δ ppm 2.13 (s, 3H), 2.27 (br. s., 4H), 2.40 (br. s., 4H), 2.64 (t, *J*=6.7 Hz, 2H), 4.09 (t, *J*=6.7 Hz, 2H), 5.75 - 5.81 (m, 1H), 6.26 (dd, *J*=16.8, 2.0 Hz, 1H), 6.42 (dd, *J*=16.8,10.2 Hz, 1H), 7.09 - 7.16 (m, 2H), 7.24 (s, 1H), 7.30 (s, 1H), 7.31 - 7.41 (m, 2H), 7.57 (t, *J*=8.0 Hz, 1H), 7.80 (t, *J*=1.9 Hz, 1H), 7.89 (dd, *J*=7.3, 1.3 Hz, 2H), 8.00 (br. s., 2H), 8.37 (s, 1H), 10.43 (s, 1H). LC-MS (M+H) 549.

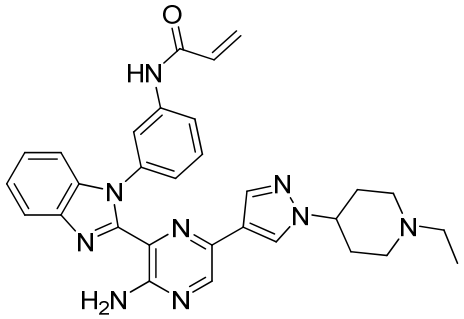

***N*-(3-(2-(3-Amino-6-(1-(1-ethylpiperidin-4-yl)-1*H*-pyrazol-4-yl)pyrazin-2-yl)-1*H*-benzo[d]imidazol-1-yl)phenyl)acrylamide (25):** ^{1}H NMR (400 MHz, DMSO-d_6) δ ppm 1.03 (t, *J*=7.5 Hz, 3H), 1.73 - 1.87 (m, 2H), 1.88 - 1.97 (m, 2H), 1.97 - 2.09 (m, 2H), 2.37 (q, *J*=7.5 Hz, 2H), 2.87 - 3.00 (m, 2H), 3.89 - 4.03 (m., 1H), 5.74 - 5.82 (m, 1H), 6.21 - 6.31 (m, 1H), 6.37 - 6.49 (m, 1H), 7.05 - 7.14 (m, 2H), 7.25 (s, 1H), 7.29 - 7.41 (m, 3H), 7.51 - 7.60 (m, 1H), 7.76 - 7.82 (m, 1H), 7.84 - 7.95 (m, 2H), 7.98 (br. s., 2H), 8.38 (s, 1H), 10.43 (s, 1H). LC-MS (M+H) 534.

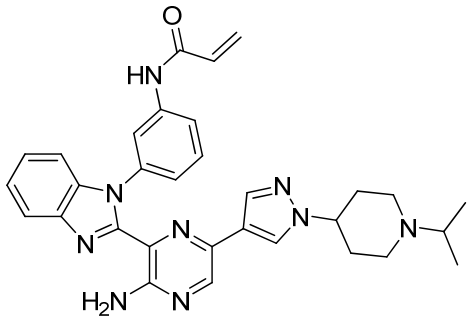

***N*-(3-(2-(3-Amino-6-(1-(1-isopropylpiperidin-4-yl)-1*H*-pyrazol-4-yl)pyrazin-2-yl)-1*H*-benzo[d]imidazol-1-yl)phenyl)acrylamide (26):** ^{1}H NMR (400 MHz, DMSO-d_6) δ ppm 1.00 (d, *J*=7.0 Hz, 6H), 1.68 - 1.83 (m, 2H), 1.87 - 1.98 (m, 2H), 2.19 - 2.31 (m, 2H), 2.75 (septet, *J*=7.0 Hz, 1H), 2.81 - 2.90 (m, 2H), 3.85 - 3.98 (m, 1H), 5.73 - 5.82 (m, 1H), 6.21 - 6.32 (m, 1H), 6.37 - 6.49 (m, 1H), 7.05 - 7.14 (m, 2H), 7.24 (s, 1H), 7.28 - 7.41 (m, 3H), 7.51

- 7.59 (m, 1H), 7.75 - 7.81 (m, 1H), 7.84 - 7.96 (m, 2H), 7.98 (br. s., 2H), 8.38 (s, 1H), 10.43 (s, 1H). LC-MS (M+H) 548.

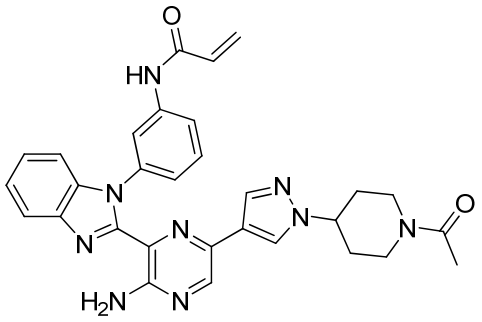

***N*-(3-(2-(6-(1-(1-Acetylpiperidin-4-yl)-1*H*-pyrazol-4-yl)-3-aminopyrazin-2-yl)-1*H*-benzo[d]imidazol-1-yl)phenyl)acrylamide (27):** ^{1}H NMR (400 MHz, DMSO-d_6) δ ppm 1.54 - 1.68 (m, 1H), 1.71 - 1.84 (m, 1H), 1.86 - 1.97 (m, 1H), 2.08 (s, 3H), 2.14 - 2.22 (m, 1H), 2.64 - 2.78 (m, 1H), 3.13 - 3.26 (m, 1H), 3.87 - 3.96 (m, 1H), 4.21 - 4.33 (m, 1H), 4.41 - 4.53 (m, 1H), 5.73 - 5.84 (m, 1H), 6.22 - 6.33 (m, 1H), 6.38 - 6.49 (m, 1H), 7.06 - 7.19 (m, 2H), 7.22 - 7.29 (m, 1H), 7.30 - 7.43 (m, 3H), 7.52 - 7.63 (m, 1H), 7.65 - 7.71 (m, 1H), 7.76 - 7.91 (m, 1H), 7.91 - 7.98 (m, 1H), 8.04 (br. s., 2H), 8.40 (s, 1H), 10.47 (s, 1H). LC-MS (M+H) 548.

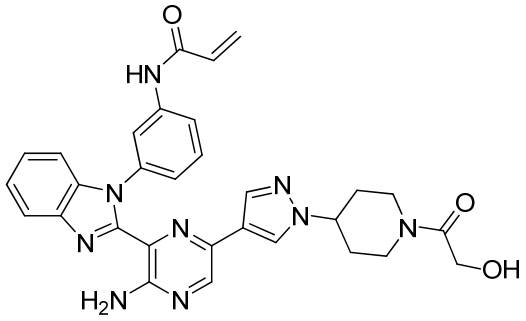

***N*-(3-(2-(3-Amino-6-(1-(1-(2-hydroxyacetyl)piperidin-4-yl)-1*H*-pyrazol-4-yl)pyrazin-2-yl)-1*H*-benzo[d]imidazol-1-yl)phenyl)acrylamide (28):** ^{1}H NMR (400 MHz, DMSO-d_6) δ ppm 1.55 - 1.70 (m, 1H), 1.70 - 1.85 (m, 1H), 1.92 - 2.06 (m, 2H), 2.75 - 2.87 (m, 1H), 3.06 -

3.20 (m, 1H), 3.69 - 3.88 (m, 1H), 4.05 - 4.34 (m, 3H), 4.40 - 4.52 (m, 1H), 4.55 - 4.65 (m, 1H), 5.71 - 5.82 (m, 1H), 6.19 - 6.30 (m, 1H), 6.38 - 6.50 (m, 1H), 7.04 - 7.16 (m, 2H), 7.23 - 7.27 (m, 1H), 7.29 - 7.40 (m, 3H), 7.51 - 7.61 (m, 1H), 7.72 - 7.81 (m, 1H), 7.84 - 7.95 (m, 2H), 8.01 (br. s., 2H), 8.38 (s, 1H), 10.44 (s, 1H). LC-MS (M+H) 564.

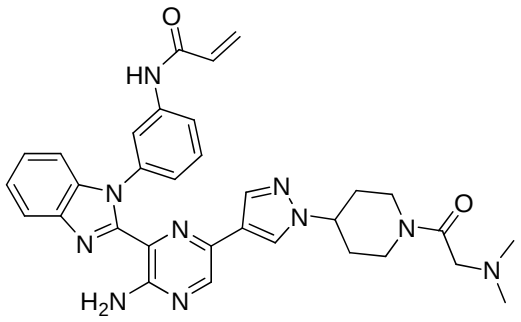

***N*-(3-(2-(3-Amino-6-(1-(1-(2-(dimethylamino)acetyl)piperidin-4-yl)-1*H*-pyrazol-4-yl)pyrazin-2-yl)-1*H*-benzo[d]imidazol-1-yl)phenyl)acrylamide (29):** ^{1}H NMR (400 MHz, DMSO-d_6) δ ppm 1.56 - 1.61 (m, 1H), 1.62 - 1.76 (m, 1H), 1.92 - 2.06 (m, 2H), 2.26 (s, 6H), 2.64 - 2.84 (m, 1H), 2.88 - 3.02 (m, 1H), 3.10 - 3.27 (m, 2H), 4.08 - 4.20 (m, 1H), 4.22 - 4.37 (m, 1H), 4.40 - 4.51 (m, 1H), 5.72 - 5.83 (m, 1H), 6.20 - 6.32 (m, 1H), 6.37 - 6.50 (m, 1H), 7.05 - 7.20 (m, 2H), 7.22 - 7.47 (m, 4H), 7.52 - 7.62 (m, 1H), 7.71 - 7.80 (m, 1H), 7.83 - 7.92 (m, 2H), 7.92 - 7.99 (m, 1H), 8.04 (br. s., 1H), 8.16 (s, 1H), 8.40 (s, 1H), 10.46 (s, 1H). LC-MS (M+H) 591.

Kinase Selectivity Data for Compounds 5 and 19:

Compounds **5** and **19** were tested (Millipore KinaseProfiler), for inhibitory activity across a panel of 125 different kinases representative of the human kinome. At a concentration of 1 μM, compound **5** inhibits the activity of 31 out of 125 kinases at greater than 50% (Gini coefficient= 0.57),[2] and 19 kinases at greater than 75%. At a concentration of 1 μM, compound **19** inhibits the activity of 52 out of 125 kinases at greater than 50% (Gini coefficient = 0.44), and 31 kinases at greater than 75%.

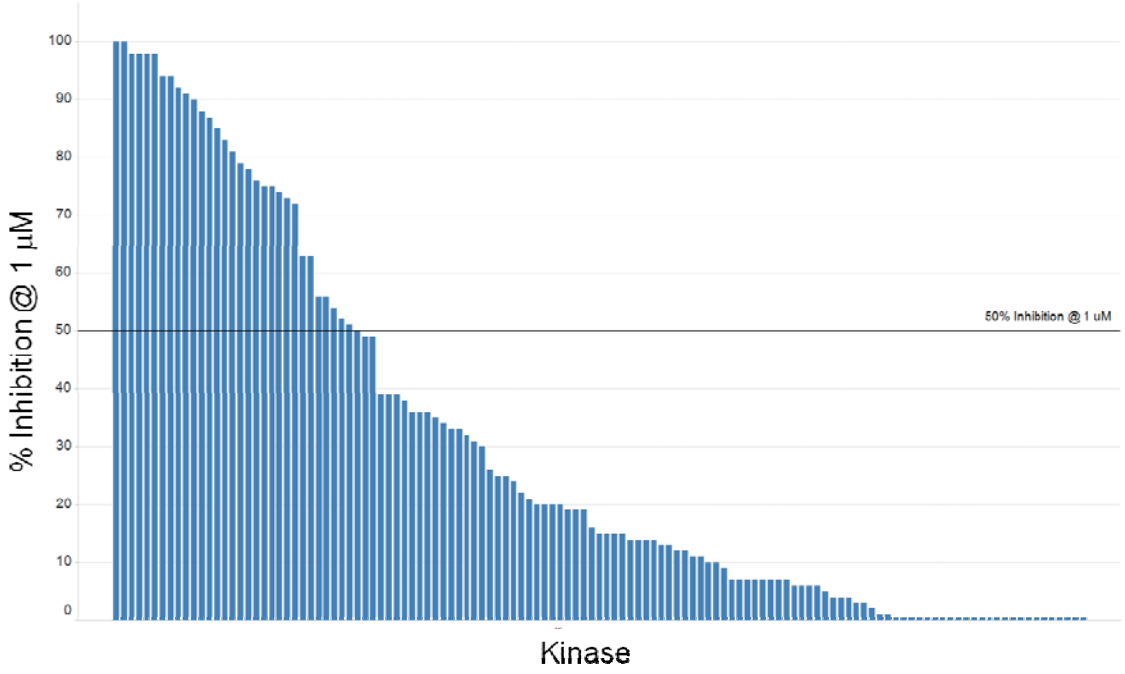

Figure S3. Kinase inhibition of compound **5** across a panel of 125 kinases.

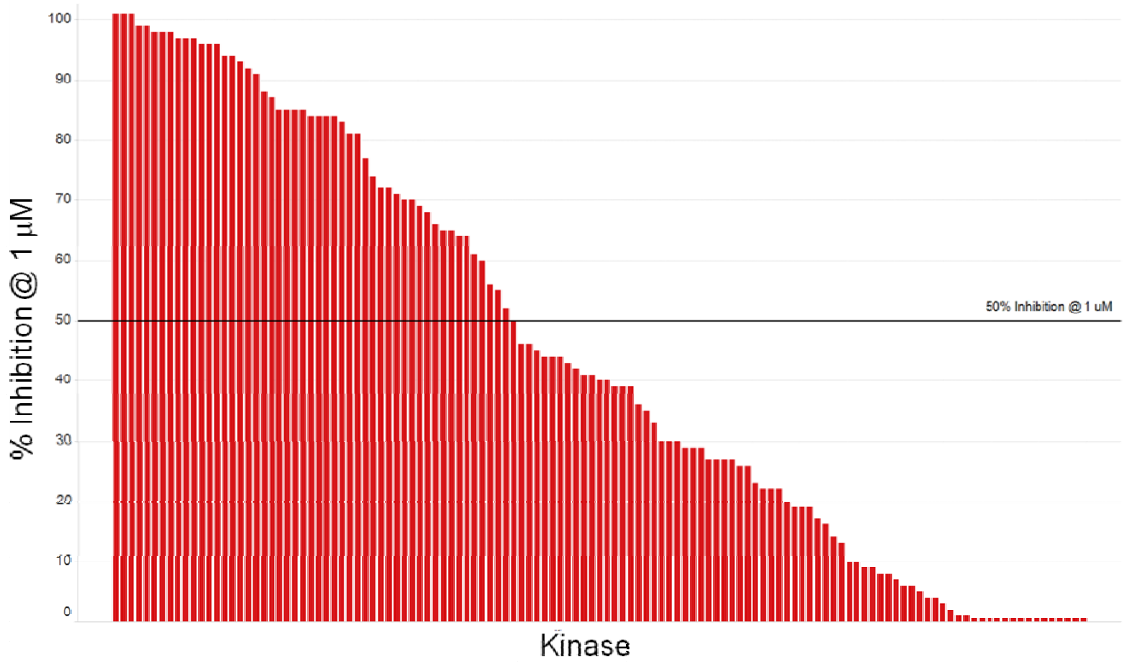

Figure S4. Kinase inhibition of compound **19** across a panel of 125 kinases.

Assessment of Compound Reactivity with Glutathione:

To determine the intrinsic reactivity of the acrylamide moiety of compounds in this paper towards thiol nucleophiles, a select group of these compounds were incubated in the presence of glutathione (GSH) and the formation of the expected adduct was measured over time. A desirable "reactivity window" has previously been defined, with compounds having half-lives of between 25 minutes and 400 minutes having suitable reactivity towards EGFR Cys797 while bound to the ATP-binding site of the kinase while avoiding promiscuous labeling of other potentially reactive proteins in cells.[3]

Fifty micromolar of compound was reacted with an excess of glutathione (4.6 mM GSH) in phosphate buffer at pH 7.4 and 37 °C for 24 h. The reaction was followed by monitoring the loss of the parent by LC−UV−MS, and the data were fitted to first-order kinetics from which the half-lives of reaction were determined. Reaction of *p*-nitrobenzylchloride (PNBC) with glutathione was used as a positive control for the assay (Log k_{GSH} −1.747 mol^{-1} s^{-1}, SD 0.077, and n = 24).

Table S1. Half-lives for the reaction of selected compounds with glutathione (GSH).

Compound	GSH $t_{1/2}$ (min)
5	44
13	114
16	122
19	44
20	63

Kinase Inhibition Assay Using HTRF (Homogenous Time-Resolved Fluorescence):

The inhibitory activity of compound against the kinase EGFR (T790M/L858R) was determined with CisBio HTRF (homogenous time-resolved fluorescence) KinEASE TK (#62TKOPEC). The enzyme reaction contains recombinant N-terminal GST-tagged human EGFR (T790M/L858R), which phosphorylates the HTRF tyrosine kinase biotinylated substrate. The sequence of the substrate is proprietary to CisBio. Compounds were serially diluted in 100% (v/v) DMSO before being acoustically dispensed from an Echo 555 (Labcyte) into black Corning 1536-well assay plates. Kinase activity assays were performed in a total reaction volume of 3 μL per well. A 1.5 μL enzyme reaction consisted of 1.6 nM EGFR (T970M, L858R), 1 mM DTT, and 10 mM $MgCl_2$. A 1.5 μL substrate mix consisted of 1 μM TK substrate, 30 μM ATP, 1 mM DTT, and 10 mM $MgCl_2$. Following a 50 min incubation, 3 μL of stop mix was added, which consisted of 250 nM Strep-XL665 and TK Ab-Cryptate diluted in kit detection buffer. The plates were incubated for 1 h before being read on Pherastar using standard HTRF settings. N-terminal GST-tagged recombinant human EGF receptor, with amino acids 696-end containing the T790M and L858R mutations, was obtained from Millipore.

Experimental Procedure for the Inhibition of Cellular Phosphorylation Assay:

For EGFR (T790M/L858R), the human lung cell line NCI-H1975 was obtained from the American Type Culture Collection. For EGFR (Exon 19 deletion), the human lung cell line PC9 was obtained from the Akiko Hiraide from Preclinical Sciences R&D AZ Japan. The growth media was RPMI 1640 containing 10% fetal calf serum and 2 mM glutamine. For EGFR (wild type), the human colon adenocarcinoma cell line LoVo was obtained from the

European Collection of Cell Cultures. LoVo growth media was RPMI 1640 containing 3% charcoal-stripped fetal calf serum and 2 mM glutamine. All cells were used from assay-ready frozen cryo banks. Assays to measure cellular phosphorylation of endogenous p-EGFR in cell lysates were carried out according to the protocol described in the R&D Systems DuoSet IC Human Phospho-EGFR ELISA (R&D Systems, no. DYC1095). Following thawing and resuspension, 40 μL of cells were seeded (10,000 cells/well for NCIH1975 and PC9 or 15,000 cells/well for LoVo) in growth medium in Corning black, clear-bottomed 384-well plates and incubated at 37 °C with 5% CO_2 overnight. The cells were acoustically dosed using an Echo 555 with compounds serially diluted in 100% DMSO (v/v). The cells were incubated for a further 2 h and following aspiration of medium, 40 μL of 1× lysis buffer was added to each well. LoVo were stimulated with EGF (25 ng/mL) for 10 min before lysis. Greiner black high-bind 384-well plates were coated with capture antibody and then blocked with 3% BSA. Following the removal of the blocking solution, 15 μL of lysate was transferred to the Greiner black high-bind 384-well plates and incubated for 2 h. Following aspiration and washing of the plates with PBS/A, 20 μL of detection antibody was added and incubated for 2 h. Following aspiration and washing of the plates with PBS/T, 20 μL of QuantaBlu fluorogenic peroxidase substrate (Thermo-Fisher Scientific, no. 15169) was added and incubated for 1 h. Twenty microliters of QuantaBlu stop solution was added to the plates, and fluorescence was read on an Envision plate reader using an excitation wavelength of 352 nm and an emission wavelength of 460 nm.

Experimental Procedure for Cellular Proliferation Experiments:

Cell lines were plated in 384−well plates at between 500 and 1000 cells per well, depending on the cell line, in 70 μL per well of RPMI media containing 10% fetal calf serum, 2 mM L-

glutamine, and 1% penicillin/streptomycin. The cells were allowed to attach overnight at 37 °C under 5% CO_2. The following day, titrations of test compound were added to the assay plates using an Echo Liquid Handler Labcyte, and the treated cells were incubated for a further 72 h at 37 °C under 5% CO_2. Each compound was tested as an 11-point dose response, with a top concentration of 10 μM using 1:3 dilutions. Following a 72 h incubation of the compound-treated plates, 5 μL of 2 μM SYTOX Green Nucleic Acid Stain, Life Technologies was added per well, and the plates were incubated at room temperature for 1 h. The number of fluorescent cells per well was measured with an Acumen TTP LabTech Ltd., with this number representing the dead cell count. Ten microliters of 0.25% saponin was added per well, and the plates were incubated overnight at room temperature. The total number of fluorescent cells per well was acquired with the Acumen. The number of dead cells was subtracted from the total number of cells, and the live cell number was plotted to determine GI_{50} values.

Pharmacokinetics of Compound 5 in Mouse

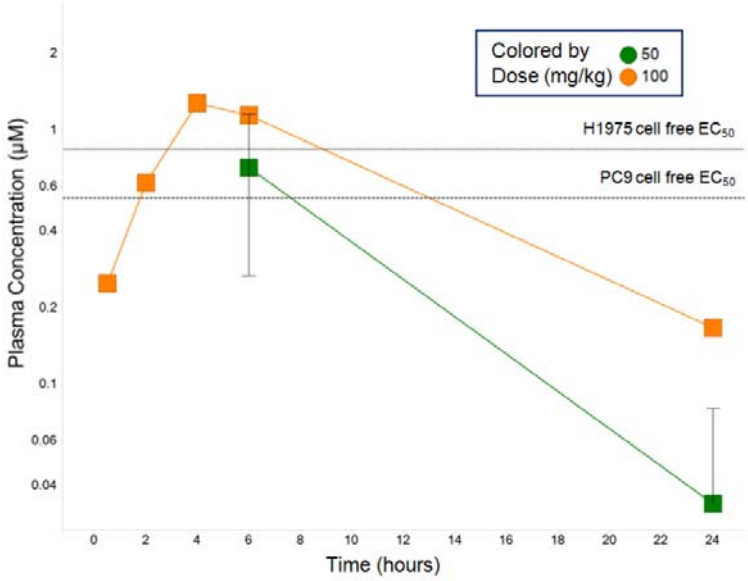

Figure S5. Plasma concentrations of compound **5** vs. time following a single oral dose given to female nude mice. Data from the 100 mg/kg dose (orange curve) is from a single animal, while the data from the 50 mg/kg dose (green curve) is the mean of data from 5 animals ± standard deviation. The horizontal lines correspond to the cellular EC_{50} values in the H1975 and PC9 cell lines, corrected for protein binding.

X-ray Crystallography Collection and Refinement Data

The human JAK3 protein sample for crystallography was produced in a baculovirus expression system as GST fusion protein and was co-crystallised with the compound as described previously.[4] Diffraction data were collected at the Swiss Light Source at cryogenic temperatures on a Pilatus6M detector, and processed using XDS.[5] The structure was solved using the molecular replacement technique with the CCP4 suite of software.[6] The crystallographic model was completed in Coot[7] and refined with Refmac5.[8] Crystallographic data and refinement parameters are summarised in Table S2. The structure was deposited in the PDB with the accession code 4V0G.

Table S2. Crystallographic data collection and refinement summary.

Data collection statistics	
Cell parameters: a, b, c [Å] α=β=γ [◦]	 57.14, 99.03, 111.37 90
Resolution [Å]	3.00 (3.24-3.00)‡
Unique reflections	13190 (2632)‡
Multiplicity	4.0 (4.0)‡
Completeness [%]	99.7 (99.1)‡
R_{sym} [%]	13.6 (44.3)‡
Mean(I)/sd	5.8 (2.1)‡

Refinement statistics	
Number of reflections (working /test)	12552 / 593
R/R_{free} [%]	25.2/29.5
Number of atoms: protein water ligand	 4382 12 78
Deviation from ideal geometry bond lengths [Å] bond angles [◦] Bonded B's [$Å^2$]	 0.007 0.99 1.5
Ramachandran plot [%] most favoured region additional allowed region generously allowed region disallowed region	 87.9 11.9 0.2 0

ǂ Data in parentheses refer to the highest resolution shell.

References

(1) Cui, J. J.; Funk, L. A.; Jia, L.; Kung, P.-P.; Meng, J. J.; Nambu, M. D.; Pairish, M. A.; Shen, H.; Tran-Dube, M. B. Pyrazole-Substituted Aminoheteroaryl Compounds as Protein Kinase Inhibitors. WIPO Patent WO2006021881, 2006.

(2) Graczyk, P. P. Gini Coefficient: A New Way To Express Selectivity of Kinase Inhibitors against a Family of Kinases. *J. Med. Chem.* **2007**, *50*, 5773-5779.

(3) Ward, R. A.; Anderton, M. J.; Ashton, S.; Bethel, P. A.; Box, M.; Butterworth, S.; Colclough, N.; Chorley, C. G.; Chuaqui, C.; Cross, D. A. E.; Dakin, L. A.; Debreczeni, J. É.; Eberlein, C.; Finlay, M. R. V.; Hill, G. B.; Grist, M.; Klinowska, T. C. M.; Lane, C.; Martin, S.; Orme, J. P.; Smith, P.; Wang, F.; Waring, M. J. Structure- and Reactivity-Based Development of Covalent Inhibitors of the Activating and Gatekeeper Mutant Forms of the Epidermal Growth Factor Receptor (EGFR). *J. Med. Chem.* **2013**, *56*, 7025-7048.

(4) Boggon, T. J.; Li, Y.; Manley, P. W.; Eck, M. J. Crystal structure of the Jak3 kinase domain in complex with a staurosporine analog. *Blood* **2005**, *106*, 996-1002.

(5) Kabsch, W. XDS. *Acta Crystallogr., Sect. D* **2010**, *66*, 125-132.

(6) Winn, M. D.; Ballard, C. C.; Cowtan, K. D.; Dodson, E. J.; Emsley, P.; Evans, P. R.; Keegan, R. M.; Krissinel, E. B.; Leslie, A. G. W.; McCoy, A.; McNicholas, S. J.; Murshudov, G. N.; Pannu, N. S.; Potterton, E. A.; Powell, H. R.; Read, R. J.; Vagin, A.; Wilson, K. S. Overview of the CCP4 suite and current developments. *Acta Crystallogr., Sect.. D* **2011**, *67*, 235-242.

(7) Emsley, P.; Lohkamp, B.; Scott, W. G.; Cowtan, K. Features and development of *Coot*. *Acta Crystallogr., Sect. D* **2010**, *66*, 486-501.

(8) Murshudov, G. B.; Vagin, A. A.; Dodson, E. J. Refinement of Macromolecular Structures by the Maximum-Likelihood Method. *Acta Crystallogr., Sect. D* **1997**, *53*, 240-255.